Journal of Mechanical Design | Volume 135 | Issue 12 | research-article

Probabilistic Inverse Simulation and its Application in Vehicle Accident Reconstruction

Xiaoyun Zhang
School of Mechanical Engineering
Shanghai Jiaotong University

Zhen Hu
Department of Mechanical and Aerospace Engineering
Missouri University of Science and Technology

Xiaoping Du[1]
Corresponding Author
Department of Mechanical and Aerospace Engineering
Missouri University of Science and Technology

[1] Corresponding author: 400 West 13th Street, Toomey Hall 290D, Rolla, MO 65401, U.S.A. Tel: 1-573-341-7249, E-mail: dux@mst.edu

AUTHORS INFORMATION:

Xiaoyun Zhang, Ph.D.

Associate Professor

School of Mechanical Engineering

Shanghai Jiaotong University

Mechanical Building, 800 Dong Chuan Road

Shanghai 200240, P.R.China

E-mail: zhangxiaoyun_sjtu@hotmail.com

Zhen Hu, M.S.

Research Assistant

Department of Mechanical and Aerospace Engineering

Missouri University of Science and Technology

290D Toomey Hall
400 West 13th Street
Rolla, MO 65409-0500
E-mail: zh4hd@mst.edu

Xiaoping Du, Ph.D.

Associate Professor

Department of Mechanical and Aerospace Engineering

Missouri University of Science and Technology

290D Toomey Hall

400 West 13th Street

Rolla, MO 65409-0500

573-341-7249 (voice)

573-341-4607 (fax)

E-mail: dux@mst.edu

Abstract

Inverse simulation is an inverse process of direct simulation. It determines unknown input variables of the direct simulation for a given set of simulation output variables. Uncertainties usually exist, making it difficult to solve inverse simulation problems. The objective of this research is to account for uncertainties in inverse simulation in order to produce high confidence in simulation results. The major approach is the use of the maximum probability density function, which determines not only unknown deterministic input variables but also the realizations of random input variables. Both types of variables are solved on the condition that the joint probability density of all the random variables is maximum. The proposed methodology is applied to a traffic accident reconstruction problem where the simulation output (accident consequences) is known and the simulation input (velocities of the vehicle at the beginning of crash) is sought.

Keywords: Inverse simulation, maximum probability, accident reconstruction, optimization

1. Introduction

Inverse simulation is an inverse process of direct simulation. During this process, computer simulations are used in an inverse way. A set of unknown model input variables are found given a set of known model output variables.

Inverse simulation has been applied in many engineering areas. For instance, it is extensively used and becomes a current research focus in the area of inverse dynamic analysis, such as determining the forces or torques so as to produce desired motions [1, 2], finding appropriate joint parameters for robots [3], and determining torques and powers for desired human movements [4-7]. The applications in aerospace engineering have also been reported, such as dynamic inversion [8], flight control [9, 10], optimization of helicopter slalom maneuver [11], and other applications [12-14].

Even though inverse simulations are intensively used for inverse dynamic analysis, they are not limited to dynamic analysis. Traffic accident reconstruction, which is the focus of this work, is another area to which inverse simulations are applied. It is different from the traditional inverse dynamics where the number of to-be-determined input variables, which enforce a dynamical system to complete the specified output, is generally equal to the number of dynamic equations. For the accident reconstruction inverse simulation, the number of unknowns may be different from that of simulation equations. Some of the input variables, such as the coefficient of friction, are not known exactly. These variables together with the totally unknown input variables, such as the pre-impact velocity, are determined by optimization so that the direct simulation result is

close to observations. Details about the inverse simulation of traffic accident reconstruction are discussed in Section 2.

Fig. 1 shows a general simulation model. The vectors of input and output variables are $\mathbf{x}$ and $\mathbf{y}$, respectively. $\mathbf{x}$ and $\mathbf{y}$ may be time independent or time dependent. The simulation model $\mathbf{g}(\mathbf{x})$ maps $\mathbf{x}$ into $\mathbf{y}$ and is given by

$$\mathbf{y} = \mathbf{g}(\mathbf{x}) \tag{1}$$

or

$$\begin{cases} y_1 = g_1(\mathbf{x}) \\ y_2 = g_2(\mathbf{x}) \\ \cdots \\ y_m = g_m(\mathbf{x}) \end{cases} \tag{2}$$

where $\mathbf{y} = (y_1, \ldots, y_m)^{\mathrm{T}}$, and $\mathbf{g}(\cdot) = (g_1(\cdot), \ldots g_m(\cdot))^{\mathrm{T}}$. We call these equations the *direct simulation equations*.

Place Fig. 1 here

For inverse simulation, the output variables $\mathbf{y}$ are known, and part of the input variables are to be determined. We use $\mathbf{x}_{\mathrm{unkn}}$ for those to-be-determined variables. Some input variables are precisely known, and we denote them by $\mathbf{x}_{\mathrm{kn}}$.

As many uncertainties are presented in the direct process of simulation [15-17], we also encounter uncertainties in inverse simulation. The uncertainties may be associated with simulation parameters that are related to the stochastic physical nature, manufacturing imprecision, random operating conditions, and measurement errors. As a result, we may not know some of the input variables precisely, and we treat them as random variables. Those random variables are denoted by $\mathbf{x}_{\mathrm{rand}}$. Model structure uncertainty also exists due to simplifications, assumptions, ignorance, and lack of information within the model. When we solve for the unknown input variables through inverse simulation, the model structure uncertainty should also be considered.

Then the input variables $\mathbf{x}$ are

$$\mathbf{x} = (\mathbf{x}_{\mathrm{unkn}}, \mathbf{x}_{\mathrm{rand}}, \mathbf{x}_{\mathrm{kn}})^{\mathrm{T}} \tag{3}$$

where

$\mathbf{x}_{\mathrm{unkn}} = (x_{\mathrm{unkn},1}, \ldots, x_{\mathrm{unkn},n_{\mathrm{unkn}}})^{\mathrm{T}}$ with a size of n_{unkn},

$\mathbf{x}_{\mathrm{rand}} = (x_{\mathrm{rand},1}, \ldots, x_{\mathrm{rand},n_{\mathrm{rand}}})^{\mathrm{T}}$ with a size of n_{rand}.

Since the precisely known variables $\mathbf{x}_{\mathrm{kn}}$ are not important in our discussions, we omit them in the simulation models. Then the models are rewritten as

$$\mathbf{y} = \mathbf{g}(\mathbf{x}) = \mathbf{g}(\mathbf{x}_{\mathrm{unkn}}, \mathbf{x}_{\mathrm{rand}}) \tag{4}$$

The general task of inverse simulation is to find unknown input variables $\mathbf{x}_{\mathrm{unkn}}$ given output variables $\mathbf{y}$ and joint probability density distribution of random input variables $\mathbf{x}_{\mathrm{rand}}$.

We then take traffic accident reconstruction as an example to further explain inverse simulation and its input variables $\mathbf{x}_{\text{unkn}}$ and $\mathbf{x}_{\text{rand}}$. From the accident scene, we may obtain useful information, such as the victim rest position, for which we can run vehicle collision simulation repeatedly until the simulated human rest position matches the observed value. The human rest position serves as one of the output variables in $\mathbf{y}$. On the other hand, the input variables may include the pre-impact velocity of the vehicle, the distance between the pedestrian and vehicle, and the coefficient of friction. If the pre-impact velocity and the distance between the pedestrian and vehicle are what should be revealed from the inverse simulation, then they belongs to unknown input variables $\mathbf{x}_{\text{unkn}}$. The coefficient of friction may also be unknown. If we have sufficient statistical data, we know its probability density beforehand. It can be treated as a random input variable, and then it belongs to $\mathbf{x}_{\text{rand}}$. If it is difficult or impossible to measure the coefficient of friction at the accident scene, its realization can be solved for during the inverse simulation. Therefore, for an accident that has occurred, the random variables $\mathbf{x}_{\text{rand}}$ could be observed or measured; in other words, their realizations exist. These realizations of $\mathbf{x}_{\text{rand}}$ are also to-be-determined unknowns.

Due to the involvement of random variables, the traditional inverse simulation method may not be effective anymore. In this work, we develop a new inverse simulation method that can determine both the unknown deterministic input variables and the realizations of unknown random input variables. The requirement of the method is that we know the direct simulation output variables and the prior distributions of the random input variables.

Vehicle accident reconstruction is an important application area of inverse simulation, and we give a brief introduction to vehicle accident reconstruction in Section 2. We then present the proposed method in Section 3 followed by an illustration example in Section 4. The method is applied in the reconstruction of a vehicle-pedestrian accident in Section 5. Conclusions and future work are discussed in Section 6.

2. Vehicle Traffic Accident Reconstruction

The whole process of a vehicle accident can be divided into three phases:

(1) Post impact: It is the starting point of the reconstruction. The model is developed with the information obtained from the accident scene.

(2) Impact: It identifies the responses of the involved vehicle, including the impact speed, impact direction, impact location, and so on.

(3) Pre-impact. It identifies the speed and trajectory of the vehicle [18].

For traffic accident reconstruction, the key issues are the investigation and analysis of the causes and consequences of vehicle collision. More specifically, a collision analysis is performed to identify contributions of major factors to the collision. These factors include the role of the drivers, vehicles, road conditions, and environment.

Traffic accident reconstruction is an inverse process of direct simulation because it reconstructs the pre-accident events given the accident consequences. Several computer programs have been developed for the reconstruction of vehicle accidents based on the information of the accident scene. The commonly used accident scene information

include vehicle or human rest position, road marks, damages and marks of vehicle or other road infrastructures, and human injuries [19]. The most typical accident reconstruction software is PC-Crash. As the software is combined with a momentum-based collision model, the accidents can be reconstructed from the point of reaction to the end position for all involved cars simultaneously.

The major objective of accident reconstruction is to identify the pre-impact velocity and trajectory at the moment of accident. Elastic-plastic deformation of the vehicle and the injury of the human body are the important information in the vehicle crash accidents. The computer simulation models available for the accident reconstruction, however, seldom consider the deformation and the injury. With the development of simulation technology, the deformation can be fully analyzed based on the finite element method or the multi-body dynamics methods. The deformation analysis plays a vital role in the reconstruction of vehicle crash accidents. In this work, the MADYMO (Mathematical Dynamic Model) is employed to study the vehicle-pedestrian impact accident. MADYMO employs the multi-body dynamics and injury biomechanics for accident simulation. It is applicable to many kinds of transportations, such as cars, motorcycles and bicycles [20]. It uses numerical algorithms to predict the motion of systems with bodies connected by kinematic joints. It is convenient to use the database of human body models developed by TNO (Netherlands Organization for Applied Science Research) and EEVC (European Experimental Vehicles Committee), including the Hybrid Ⅲ dummy and pedestrian models in this software.

As many uncertainties present in the process of direct simulations [16, 17, 21], we also face uncertainties in inverse simulations. The uncertainties may come from simulation parameters, such as the random road conditions. They can also come from the model structure uncertainties in the vehicle crash simulation models due to simplifications, assumptions, ignorance, and lack of information. For example, there are many sources of uncertainty in traffic accident reconstruction as reported in [22, 23]. The major objective of this work is to develop a probabilistic inverse simulation methodology and then use it to deal with the uncertainties in the vehicle accident inverse simulation.

3. Inverse Simulation with Maximum Probability Density

In this section, we present the proposed methodology for inverse simulation under uncertainty. As discussed previously, the task is to find the unknown input variables $\mathbf{x}_{\mathrm{unkn}}$ given the output variables $\mathbf{y}$ and the joint probability density function of random input variables $\mathbf{x}_{\mathrm{rand}}$.

During the inverse simulation process, we need to solve the direct simulation equations in Eq. (2), and the equations with the input variables we defined in Section 1 are rewritten below.

$$\begin{cases} y_1 = g_1(\mathbf{x}_{\mathrm{unkn}}, \mathbf{x}_{\mathrm{rand}}) \\ y_2 = g_2(\mathbf{x}_{\mathrm{unkn}}, \mathbf{x}_{\mathrm{rand}}) \\ \cdots \\ y_m = g_m(\mathbf{x}_{\mathrm{unkn}}, \mathbf{x}_{\mathrm{rand}}) \end{cases} \tag{5}$$

For a special case where the dimension of $\mathbf{y}$ is equal to that of $\mathbf{x}_{\text{unkn}}$, the number of equations are equal to the number of unknown variables. Then there may be a unique solution to $\mathbf{x}_{\text{rand}}$ given a specific set of values of $\mathbf{y}$. In this case, $\mathbf{x}_{\text{unkn}}$ can be obtained with a reliability approach [24]. In this work, we discuss general problems where the number of unknowns is greater than the number of simulation equations.

The distributions of random input variables $\mathbf{x}_{\text{rand}}$ are usually obtained from statistical data, engineering judgment, and prior similar simulation applications. As discussed in Section 1, however, for a specific event under simulation, the random input variables $\mathbf{x}_{\text{rand}}$ actually become deterministic, meaning that their values are no longer random. Instead, their values are fixed but maybe unknown. For example, in a vehicle accident simulation, the coefficient of friction μ_f between the tires of the vehicle and ground might be an input random variable. When we build the simulation model for vehicle collision, we can treat μ_f as a random variable because we know there is uncertainty associate with μ_f whose distribution may be known in advance. However, for a specific accident, a unique true value of μ_f exists even though we may not know it unless we measure it. For a specific accident event, the true value of μ_f is a realization of the random variable μ_f. For this reason, the total number of unknowns in the inverse simulation is the sum of the numbers of $\mathbf{x}_{\text{unkn}}$ and $\mathbf{x}_{\text{rand}}$, or $n_{\text{unkn}} + n_{\text{rand}}$. If the number of output variables $n_y < n_{\text{unkn}} + n_{\text{rand}}$, we will have an infinite number of solutions.

To solve this problem, we need to use the prior probabilistic information about the random input variables $\mathbf{x}_{\text{rand}}$, which can in turn impose conditions in addition to the direct

simulation equations. This may allow us to generate a unique solution. Suppose the solution to the inverse simulation is $\mathbf{x}^*$, the strategy we propose is to produce the highest probability density for the random input variables $\mathbf{x}_{\mathrm{rand}}$ at $\mathbf{x}^*$. In other words, we select a solution among the infinite number of solutions so that the probability density of $\mathbf{x}_{\mathrm{rand}}$ is maximum.

The new method has a number of advantages. First, it uses all the information available. It does not simply treat $\mathbf{x}_{\mathrm{rand}}$ as unrelated unknowns; instead, the probabilistic information of $\mathbf{x}_{\mathrm{rand}}$ is fully used, and the correlation of the elements in $\mathbf{x}_{\mathrm{rand}}$ is also considered through the joint probability density of $\mathbf{x}_{\mathrm{rand}}$ and the direct simulation equations. Second, the maximum joint probability density is achieved, resulting in the highest confidence in the inverse simulation result. Third, a unique solution may be obtained. As will be discussed next, the last advantage of the new method is that the inverse simulation and probabilistic analysis can be integrated by an optimization framework, which results in an easy numerical implementation.

Let the joint probability density function (PDF) of $\mathbf{x}_{\mathrm{rand}}$ be $f(\mathbf{x}_{\mathrm{rand}})$. For a special case where all the random variables in $\mathbf{x}_{\mathrm{rand}}$ are independent, $f(\mathbf{x}_{\mathrm{rand}})$ is given by

$$f(\mathbf{x}_{\mathrm{rand}}) = \prod_{i=1}^{n_{\mathrm{rand}}} f_i(x_{\mathrm{rand},i}) \tag{6}$$

where $f_i(\cdot)$ is the PDF of $x_{\mathrm{rand},i}$.

Our task now is to find the unknown variables $\mathbf{x} = (\mathbf{x}_{\text{unkn}}^{\text{T}}, \mathbf{x}_{\text{rand}}^{\text{T}})^{\text{T}}$ that maximize $f(\mathbf{x}_{\text{rand}})$ subject to the constraints given by the direct simulation equations. We therefore establish the following optimization model:

$$\begin{cases} \max\limits_{(\mathbf{x}_{\text{unkn}}, \mathbf{x}_{\text{rand}})} f(\mathbf{x}_{\text{rand}}) \\ \text{subject to} \\ \mathbf{y} = \mathbf{g}(\mathbf{x}_{\text{unkn}}, \mathbf{x}_{\text{rand}}) \end{cases} \tag{7}$$

This model guarantees that all the direct simulation equations are satisfied while the joint probability density is maximized. The optimization model can be solved numerically. During the iterative numerical process, the direct simulation $\mathbf{y} = \mathbf{g}(\mathbf{x}_{\text{unkn}}, \mathbf{x}_{\text{rand}})$ is called repeatedly.

In many applications, the modeling errors of simulation models $\mathbf{y} = \mathbf{g}(\mathbf{x}_{\text{unkn}}, \mathbf{x}_{\text{rand}})$ are inevitable. The discrepancy between the model predictions $\mathbf{y}$ and the reality that the model reflects is the model error or model structure uncertainty. It is a difficult task to estimate the model error, and quantifying the model error is an on-going research topic. For instance, Chen et. al [25] proposed a model validation approach via uncertainty propagation and data transformation. In their method, the number of physical tests at each design setting is reduced to one by shifting the evaluation effort to probabilistic simulations. Liu et. al [26] investigated the advantages and disadvantages of various model validation metrics and then provided guidelines for choosing appropriate validation metrics in engineering applications. To assess and improve the predictive capability of computational models, Youn et. al [27] developed a hierarchical framework

for statistical model calibration. An optimization technique is integrated with the eigenvector dimension reduction (EDR) method in their approach, which maximizes the likelihood function in determining the unknown model variables. Many other efforts for quantifying model error under uncertainties can be found in [25, 26, 28-33].

The proposed inverse simulation model can also accommodate model structure uncertainty, which may be treated with a probabilistic or non-probabilistic method. Model structure uncertainty is an on-going research topic, and no mature methodologies of model structure uncertainty are available. In this work, we consider model structure uncertainty in a non-probabilistic way where intervals are used to describe model structure uncertainty. Specifically, we express the model structure uncertainty as an interval; the discrepancy between simulation result and the reality that is simulated is assumed within the interval. In fact, many simulation software vendors also provide simple bounds of the potential simulation errors.

After accommodating the model structure error in an interval format, we modify the above inverse simulation model as follows:

$$\begin{cases} \max\limits_{(\mathbf{x}_{\text{unkn}}, \mathbf{x}_{\text{rand}})} f(\mathbf{x}_{\text{rand}}) \\ \text{subject to} \\ (1-\varepsilon_1)y_1 \le g_1(\mathbf{x}_{\text{unkn}}, \mathbf{x}_{\text{rand}}) \le (1+\varepsilon_1)y_1 \\ (1-\varepsilon_2)y_2 \le g_2(\mathbf{x}_{\text{unkn}}, \mathbf{x}_{\text{rand}}) \le (1+\varepsilon_2)y_2 \\ \cdots \\ (1-\varepsilon_m)y_m \le g_m(\mathbf{x}_{\text{unkn}}, \mathbf{x}_{\text{rand}}) \le (1+\varepsilon_m)y_m \end{cases} \tag{8}$$

where ε_i is the relative error of simulation output y_i. If the model structure error is neglected, we set the model error $\varepsilon = 0$. The above model is then reduced to the model in Eq. (7). It should be noted that the solution to Eq. (8) may not be the true values for a given accident. We have the highest confident, however, on the solution because it produces the highest likelihood or probability density from optimization.

Next we discuss an important special case where all the random input variables are independently and normally distributed. This special case is important because the non-Gaussian and dependent random variables can be transformed into independently standard normal variables [34-36].

Let the mean and standard deviation of $x_{\text{rand},i}$ be μ_i and σ_i, respectively. The probability density function (PDF) of $x_{\text{rand},i}$ is

$$f_i(x_{\text{rand},i}) = \frac{1}{2\sigma_i}\exp\left[-\frac{1}{2}\left(\frac{x_{\text{rand},i}-\mu_i}{\sigma_i}\right)^2\right] \tag{9}$$

The joint PDF of $\mathbf{x}_{\text{rand}}$ is then given by

$$f(\mathbf{x}_{\text{rand}}) = \prod_{i=1}^{n_{\text{rand}}}\frac{1}{2\sigma_i}\exp\left[-\frac{1}{2}\left(\frac{x_{\text{rand},i}-\mu_i}{\sigma_i}\right)^2\right] \tag{10}$$

We transform $x_{\text{rand},i}$ into a standard normal variable u_i by

$$x_{\text{rand},i} = \mu_i + \sigma_i u_i \tag{11}$$

or

$$\mathbf{x}_{\text{rand}} = \boldsymbol{\mu} + \boldsymbol{\sigma}\mathbf{u}^{\text{T}} \tag{12}$$

where $\boldsymbol{\mu} = (\mu_1, \ldots, \mu_{n_{\text{rand}}})^{\text{T}}$ and $\boldsymbol{\sigma} = (\sigma_1, \ldots, \sigma_{n_{\text{rand}}})^{\text{T}}$.

The PDF of u_i is

$$\phi(u_i) = \frac{1}{2}\exp\left(-\frac{1}{2}u_i^2\right) \tag{13}$$

which yields the joint PDF of $\mathbf{u}$ as follows:

$$\phi(\mathbf{u}) = \frac{1}{2}\exp\left(-\frac{1}{2}\sum_{i=1}^{n_{\text{rand}}} u_i^2\right) \tag{14}$$

Maximizing the joint PDF $\phi(\mathbf{u}) = \frac{1}{2}\exp\left(-\frac{1}{2}\sum_{i=1}^{n_{\text{rand}}} u_i^2\right)$ is equivalent to minimizing $\sum_{i=1}^{n_{\text{rand}}} u_i^2$ or to minimizing $\prod_{i=1}^{n_{\text{rand}}}\left(\frac{x_{\text{rand},i} - \mu_i}{\sigma_i}\right)^2$. Then for this special case, the inverse simulation model becomes

$$\begin{cases} \min\limits_{(\mathbf{x}_{\text{unkn}}, \mathbf{u})} \sum\limits_{i=1}^{n_{\text{rand}}} u_i^2 \\ \text{subject to} \\ (1-\varepsilon_1)y_1 \le g_1(\mathbf{x}_{\text{unkn}}, \boldsymbol{\mu} + \boldsymbol{\sigma}\mathbf{u}^{\text{T}}) \le (1+\varepsilon_1)y_1 \\ (1-\varepsilon_2)y_2 \le g_2(\mathbf{x}_{\text{unkn}}, \boldsymbol{\mu} + \boldsymbol{\sigma}\mathbf{u}^{\text{T}}) \le (1+\varepsilon_2)y_2 \\ \ldots \\ (1-\varepsilon_m)y_m \le g_m(\mathbf{x}_{\text{unkn}}, \boldsymbol{\mu} + \boldsymbol{\sigma}\mathbf{u}^{\text{T}}) \le (1+\varepsilon_m)y_m \end{cases} \tag{15}$$

Let the solution be $\mathbf{u}^*$, and the realizations of $\mathbf{x}_{\text{rand}}$ are then

$$\mathbf{x}_{\text{rand}}^* = \boldsymbol{\mu} + \boldsymbol{\sigma}(\mathbf{u}^*)^{\text{T}} \tag{16}$$

For a general problem involving non-normally and dependently distributed random variables, the transformation from $\mathbf{x}_{\text{rand}}$ to $\mathbf{u}$ is also possible. For example, we can use the Rosenblatt Transformation for this task [37]. After the transformation, the model in Eq. (17) is still applicable for general inverse simulations.

With the involvement of optimization, the proposed inverse simulation is more computationally intensive than the direct simulation. The latter is repeatedly called during the optimization. The number of direct simulations is equal to the number of constraint function calls required by the inverse simulation optimization.

4. A Simple Example

Now we provide a simple example to illustrate how to implement the proposed methodology. Suppose the direct simulation equations are

$$\begin{cases} y_1 = g_1(\mathbf{x}_{\text{unkn}}, \mathbf{x}_{\text{rand}}) = x_{\text{unkn}} + x_{\text{rand},1} + x_{\text{rand},2} \\ y_2 = g_2(\mathbf{x}_{\text{unkn}}, \mathbf{x}_{\text{rand}}) = x_{\text{unkn}} + 2x_{\text{rand},1} + 3x_{\text{rand},2} \end{cases} \tag{17}$$

As indicated in Eq. (17), there are two output variables, one unknown deterministic input variable, and two random input variables. We assume that the two random variables are independent. The two output variables and distributions of the two random input variables are given in Table 1.

Place Table 1 here

For this simple problem, we do not consider the model structure uncertainty. Using Eq. (15), we obtain the inverse simulation model as

$$\begin{cases} \min\limits_{(x_{\text{unkn}},u_1,u_2)} u_1^2+u_2^2 \\ \text{subject to} \\ g_1(x_{\text{unkn}},\mu_1+\sigma_1u_1,\mu_2+\sigma_2u_2)=y_1 \\ g_2(x_{\text{unkn}},\mu_1+\sigma_1u_1,\mu_2+\sigma_2u_2)=y_2 \end{cases} \tag{18}$$

Since the direct simulation equations or the constraint functions in this example are linear, we can easily obtain an analytical solution without using any numerical procedure. The two constraint functions are

$$\begin{cases} x_{\text{unkn}}+(\mu_1+\sigma_1u_1)+(\mu_2+\sigma_2u_2)=y_1 \\ x_{\text{unkn}}+2(\mu_1+\sigma_1u_1)+3(\mu_2+\sigma_2u_2)=y_2 \end{cases} \tag{19}$$

Plugging the information in Tables 1 into the two equations, we obtain

$$\begin{cases} x_{\text{unkn}}+0.5(u_1+u_2)=-1 \\ x_{\text{unkn}}+u_1+1.5u_2=0 \end{cases} \tag{20}$$

Eliminating x_{unkn} yields

$$u_1+2u_2=2 \tag{21}$$

Or

$$u_1=2-2u_2 \tag{22}$$

Then the inverse simulation model becomes

$$\min\left(u_1^2+u_2^2\right)=\min\left[(2-2u_2)^2+u_2^2\right] \tag{23}$$

Let $W=(2-2u_2)^2+u_2^2$, and from

$$\frac{dW}{du_2}=2(2-2u_2)(-2)+2u_2=0 \tag{24}$$

we have $u_2^*=0.8$, which results in $u_1^*=2-2u_2^*=0.4$ and $x_{\text{unkn}}=-1.6$. Given the simulation output $y_1=1$ and $y_2=5$, with the highest probability density, we obtain the unknown input variable $x_{\text{unkn}}=-1.6$, as well as the realizations of the two random input variables in the transformed space $u_1^*=0.4$ and $u_2^*=0.8$. The latter two variables produce the highest probability density on the condition that all the direct simulation equations are satisfied. Fig. 2 shows that the joint probability density of u_1 and u_2 in the transformed space, as well as the two direct simulation equations. The figure clearly indicates that at $u_1^*=0.4$ and $u_2^*=0.8$ the joint probability density reaches its maximum.

The realizations of the random variables in the original space are

$$x_{\text{rand},1}^*=\mu_1+\sigma_1u_1^*=1+0.5u_1^*=1.2 \tag{25}$$

and

$$x_{\text{rand},2}^*=\mu_2+\sigma_2u_2^*=1+0.5u_2^*=1.4 \tag{26}$$

Through this simple example, we demonstrated the key concept of the proposed inverse simulation method and its implementation. No numerical algorithm was used to solve the optimization problem. However, in real engineering applications, the direct simulation equations are much more complicated. As will be shown in the vehicle

accident reconstruction example, a numerical algorithm is necessary for solving the inverse simulation optimization.

Place Fig. 2 here

---

5. Application in Vehicle Traffic Accident Reconstruction

In this section, we apply the proposed inverse simulation method in vehicle traffic accident reconstruction.

5.1. Problem statement

The case was documented in the accident database at the Traffic Police Brigade of Shanghai Municipal Public Security Bureau. The case collected contains detailed information regarding the vehicle, victim and environment involved in the accident.

The accident occurred on a street in Shanghai, China, in September 2009. A female pedestrian was struck by a car when she was walking across the street. The pedestrian sustained comminuted fracture to both of her tibia and fibula.

According to the vehicle inspection and forensic reports, the front of the car hit the pedestrian on her left side. The deformation of the vehicle was found at the bumper and the windscreen, as shown in Figs. 3 and 4, respectively. The first collision point was identified with the tire marks on the road. The victim fell on the road with the

pedestrian's head towards east and feet towards west. The rest position of the pedestrian was estimated based on the blood marks on the road.

Place Figs. 3-4 here

5.2. Direct crash simulation

To reconstruct the car-to-pedestrian collision in an accurate and efficient way, we used multi-body dynamics simulation. The vehicle is simplified as a multi-rigid body composed of the bumper, front lights, auto-body, windscreen, and wheels. The body movement and rotation were modeled as free hinges. The shape and mass of the vehicle model was built with the information from the aforementioned official documents.

A MADAYMO dummy model by TNO (Netherlands Organization for Applied Science Research) was adopted as the pedestrian model for simulation. The model was scaled and its mass distribution was adjusted so that the simulated pedestrian would be as realistic as possible. Fig. 5 shows the 3D simulation model of the accident scene.

Place Fig. 5 here

The simulation parameters are indicated in Fig. 6. The position parameter of the pedestrian is *d*, which is the distance between the pedestrian's mass center and the

vehicle midline. v is the pre-impact velocity of the vehicle. According to the statement of the driver, the pedestrian was noticed when she was very close to the car. Due to the high speed, the driver applied the brake gently and steered to the right side. He jammed the brake immediately after the pedestrian was hit. The brake was not released until the car stopped. The laboratory experiment revealed that the braking time of the car was 0.99 s, meaning that it took 0.99 s for the brake to be effective.

Place Fig. 6 here

The known input variables include the mass of the car and that of the pedestrian, and the movement direction of the car. The unknown input variables are the pre-impact velocity of the car *v*. The lateral distance between the pedestrian's mass center and the vehicle midline *d* is estimated according to the accident scene. To account for the errors in the estimation, it is assumed to be a random input variable. The coefficient of kinetic friction μ_k is also treated as a random input variable. Then, we have $\mathbf{x}_{\mathrm{unkn}} = v$, and $\mathbf{x}_{\mathrm{rand}} = (d, \mu_k)^T$. The outputs of the simulation include the rest position coordinates of the pedestrian (s_x, s_y), and therefore $\mathbf{y} = (s_x, s_y)^T$. From the measurements at the accidence scene, we have $\mathbf{y} = (s_x, s_y)^T = (9.59, 17.02)^T$ m.

For the multi-body simulation, two constraints should be met to ensure that the results are reasonable for a real collision accident. The first constraint is that the input variables are restricted in specified ranges. The other constraint is the simulation results

should be consistent with those from field investigation. For example, the rest point of the pedestrian, the injury of human, and the deformation of the auto-body. It only took only 3.2 seconds for the collision accident to happen. Each simulation of the accident, however, cost about 40 to 50 minutes. Fig. 7 shows one example of the simulated accident in the form of animation.

Place Fig. 7 here

5.3. Construction of surrogate models

As discussed in the last subsection, the direct simulation of the vehicle crash accident is very time consuming. Directly using the crash simulation is costly for the inverse simulation of the accident reconstruction. To this end, building surrogate models for the direct simulate equations is necessary. A surrogate model is an approximation to the original simulation model. If a surrogate model is carefully constructed, good accuracy can be maintained with much higher efficiency. Surrogate models are intensively used in engineering applications. Since surrogate models are explicit and computationally cheaper, they make inverse simulation under uncertainty much more efficient.

The surrogate models of s_x and s_y (output) are functions of input variables, including the vehicle speed v, the distance d, and the coefficient of kinetic friction μ_k.

With our experience in vehicle accident simulation, we bounded the speed v on the interval of [40, 100] km/h and treated d and μ_k as normally distributed random variables. The input variables are summarized in Table 2.

Place Table 2 here

As d and μ_k are presented as random variables and v is bounded in an interval, we used the polynomial chaos expansion (PCE) [38, 39] method to construct the surrogate models. In the PCE method, we expanded v using the Legendre polynomial bases and d and μ_k using the Hermit polynomial bases. The surrogate models were constructed by the following procedures:

- Generate samples for v, d, and μ_k using the Hammersley Sampling (HS) [40] method.
- Perform vehicle accident simulations at the sampling points of v, d, and μ_k and obtain s_x and s_y.
- Compute the coefficients of the surrogate models using the point collocation method.
- Construct the surrogate models with coefficient obtained.

Table 3 presents the samples and simulation results for the traffic accident reconstruction problem.

The constructed surrogate models for s_x and s_y are given by

$$s_x = g_1(v, d, \mu_k) = \sum_{k=0}^{19} \chi_k^x \Gamma_k(\xi) = \sum_{i=0}^{3} \sum_{j=0}^{3-i} \sum_{k=0}^{3-i-j} \chi_{(i,j,k)}^x L_i(\xi_1) H_j(\xi_2) H_k(\xi_3) \tag{27}$$

$$s_y = g_2(v, d, \mu_k) = \sum_{k=0}^{19} \chi_k^y \Gamma_k(\xi) = \sum_{i=0}^{3} \sum_{j=0}^{3-i} \sum_{k=0}^{3-i-j} \chi_{(i,j,k)}^y L_i(\xi_1) H_j(\xi_2) H_k(\xi_3) \tag{28}$$

$$\xi_1 = \frac{d - \mu_d}{\sigma_d}, \xi_2 = \frac{\mu_k - \mu_\mu}{\sigma_\mu} \tag{29}$$

and

$$\xi_3 = \frac{2v - v_L - v_U}{v_U - v_L} \tag{30}$$

where

— $H_i(\cdot)$, where $i = 0,1,2,3$, is the *i*-th order Hermit polynomial basis

— $L_i(\cdot)$, where $i = 0,1,2,3$, is the *i*-th order Legendre polynomial basis

— $v_L = 40$ km/h and $v_U = 100$ km/h are the lower and upper bounds of the vehicle speed, respectively

---

Place Table 3 here

The coefficients of the surrogate models are given as follows:

$$
\begin{aligned}
&\chi^{x}_{(0,0,0)} = 10.597,\ \chi^{x}_{(0,0,1)} = -5.699,\ \chi^{x}_{(0,0,2)} = -1.686,\ \chi^{x}_{(0,0,3)} = -1.089,\ \chi^{x}_{(0,1,0)} = -6.870,\\
&\chi^{x}_{(0,1,1)} = -2.903,\ \chi^{x}_{(0,1,2)} = -2.465,\ \chi^{x}_{(0,2,0)} = -3.070,\ \chi^{x}_{(0,2,1)} = 1.069,\ \chi^{x}_{(0,3,0)} = -1.969,\\
&\chi^{x}_{(1,0,0)} = -12.483,\ \chi^{x}_{(1,0,1)} = 6.029,\ \chi^{x}_{(1,0,2)} = 2.681,\ \chi^{x}_{(1,1,0)} = -0.584,\ \chi^{x}_{(1,1,1)} = 3.805,\\
&\chi^{x}_{(1,2,0)} = 3.371,\ \chi^{x}_{(2,0,0)} = 0.402,\ \chi^{x}_{(2,0,1)} = -3.365,\ \chi^{x}_{(2,1,0)} = -1.726,\ \chi^{x}_{(3,0,0)} = 0.130
\end{aligned}
\tag{31}
$$

and

$$
\begin{aligned}
&\chi^{y}_{(0,0,0)} = 12.201,\ \chi^{y}_{(0,0,1)} = -0.068,\ \chi^{y}_{(0,0,2)} = 0.357,\ \chi^{y}_{(0,0,3)} = -0.447,\ \chi^{y}_{(0,1,0)} = 2.614,\\
&\chi^{y}_{(0,1,1)} = 0.210,\ \chi^{y}_{(0,1,2)} = 2.270,\ \chi^{y}_{(0,2,0)} = 0.075,\ \chi^{y}_{(0,2,1)} = -0.378,\ \chi^{y}_{(0,3,0)} = 0.077,\\
&\chi^{y}_{(1,0,0)} = -2.861,\ \chi^{y}_{(1,0,1)} = 1.221,\ \chi^{y}_{(1,0,2)} = 0.511,\ \chi^{y}_{(1,1,0)} = -3.350,\ \chi^{y}_{(1,1,1)} = 3.499,\\
&\chi^{y}_{(1,2,0)} = -4.077,\ \chi^{y}_{(2,0,0)} = -1.491,\ \chi^{y}_{(2,0,1)} = 1.153,\ \chi^{y}_{(2,1,0)} = -0.177,\ \chi^{y}_{(3,0,0)} = 0.598
\end{aligned}
\tag{32}
$$

5.4. Inverse simulation

Applying the proposed inverse simulation model in Eq. (15), we obtained the following model for the traffic accident reconstruction:

$$
\begin{cases}
\underset{v,u_1,u_2}{\text{Min}} \ \sum_{i=1}^{2} u_i^2 \\
\text{Subject to} \\
\xi_1 = u_1,\ \xi_2 = u_2 \\
\xi_3 = \dfrac{2v - v_L - v_U}{v_U - v_L} \\
s_x^*(1-\varepsilon_x) \le \sum_{i=0}^{3}\sum_{j=0}^{3-i}\sum_{k=0}^{3-i-j} \chi^{x}_{(i,j,k)} L_i(\xi_1) H_j(\xi_2) H_k(\xi_3) \le s_x^*(1+\varepsilon_x) \\
s_y^*(1-\varepsilon_y) \le \sum_{i=0}^{3}\sum_{j=0}^{3-i}\sum_{k=0}^{3-i-j} \chi^{y}_{(i,j,k)} L_i(\xi_1) H_j(\xi_2) H_k(\xi_3) \le s_y^*(1+\varepsilon_y)
\end{cases}
\tag{33}
$$

where u_1 and u_2 are realizations of standard normal variables associated with the random input variables d and μ_k, and ε_x and ε_x represent the relative model errors. With our

experience in vehicle accident simulation, as well as the error of the surrogate models, we set $\varepsilon_x = \varepsilon_y = 5\% = 0.05$. The direct simulation output variables were measured from the accident scene, and they were $\mathbf{y} = (s_x, s_y)^T = (9.59, 17.02)^T$ m.

Solving Eq. (33), we obtained the results $v^* = 68.98$ km/h, $d^* = 0.59$ m, and $\mu_k^* = 0.8054$ with the highest probability density. The predicted vehicle velocity right before collision was therefore 68.98 km/h. This prediction is close to the observed velocity from the video record. The observed velocity was estimated over an interval of [67, 69] km/h. The result indicates the feasibility of the proposed method in identifying unknown variables in inverse simulation under uncertainty.

After obtaining the results, v^*, d^*, and μ^*, we conducted further investigations. Inputting v^*, d^*, and μ^* into the direct accident simulation model, we gained better understanding about the relationship between the injury of the pedestrian and the deformation of the vehicle body as shown in Fig. 8.

The data of the pedestrian's injury can be obtained by the numerical method. The acceleration curve of the pedestrian's head is plotted in Figs. 9. It indicates that the head has been struck at least 4 times, the first two strikes being the most severe. The head hit the windscreen and then the ground at two specific moments. In addition to the two fatal injuries on the head, we also investigated the other two injuries, which were not severe. Simulation results suggested that the tibia and fibula fractures were caused by the strike at the very beginning when the pedestrian was hit by the bumper. The lateral torque curve

of the pedestrian's lower limbs is plotted in Figs. 10. This is also compatible with the forensic examination.

Place Figs. 8-10 here

---

6. Conclusions

Uncertainties exist in both parameters and model structures in almost all the inverse simulations. Considering uncertainties in inverse simulation will increase the confidence of the inverse simulation results. This work employs the maximum probability density function to predict unknown model input variables, as well as the realizations of random input variables whose prior joint probability density functions are known, given that the simulation output variables are observed. The proposed probabilistic inverse simulation method is implemented by an optimization process where the joint probability density of the random input variables is maximized while the constraints of the direct simulation equations are maintained. The application of the proposed method in a vehicle accident reconstruction indicates the effectiveness of the method.

Using optimization to maximize the probability density, the proposed method can produce a unique solution to an inverse simulation problem. The solution may not contain the true values for a given vehicle accident, and there might be multiple solutions that realize the given vehicle accident (or a given set of simulation output variables). But we

have the highest confidence on the solution from the proposed method because it produces the highest probability density. To obtain multiple solutions, we may resort to an alternative method that uses conditional probabilities. For example, for the coefficient of friction in the application of this work, we could identify its probability density on conditional of the observed accident consequences, and we could also obtain its conditional mean, variance, and other characteristics. This way we will be able to obtain a family of solutions to a given set of simulation results. Our future work will test this alternative method and compare it with the present method.

Acknowledgement

We gratefully acknowledge the Institute of Forensic Science of the Ministry of the Justice of China and the Traffic Police Brigade of Shanghai Municipal Public Security Bureau for collecting the real-world data. The first author would like to acknowledge the support from the China Scholarship Council for his stay at the Missouri University of Science and Technology as a Visiting Scholar and the support from the National Natural Science Foundation of China under grants No. 50705058 and 60970049. The last two authors would like to thank the support from the National Science Foundation through Grant CMMI 1234855 and the Intelligent Systems Center (ISC) at the Missouri University of Science and Technology.

References

[1] Pontonnier, C., and Dumont, G., 2009, "Inverse Dynamics Method Using Optimization Techniques for the Estimation of Muscles Forces Involved in the Elbow Motion," International Journal on Interactive Design and Manufacturing, 3(4), pp. 227-236.

[2] Tsai, M. S., and Yuan, W. H., 2010, "Inverse Dynamics Analysis for a 3-Prs Parallel Mechanism Based on a Special Decomposition of the Reaction Forces," Mechanism and Machine Theory, 45(11), pp. 1491-1508.

[3] Paul, R. P., 1981, *Robot Manipulators: Mathematics, Programming, and Control: The Computer Control of Robot Manipulators*, The MIT Press,

[4] Happee, R., 1994, "Inverse Dynamic Optimization Including Muscular Dynamics, a New Simulation Method Applied to Goal Directed Movements," Journal of Biomechanics, 27(7), pp. 953-960.

[5] Blajer, W., and Czaplicki, A., 2001, "Modeling and Inverse Simulation of Somersaults on the Trampoline," Journal of Biomechanics, 34(12), pp. 1619-1629.

[6] Crolet, J. M., Aoubiza, B., and Meunier, A., 1993, "Compact Bone: Numerical Simulation of Mechanical Characteristics," Journal of Biomechanics, 26(6), pp. 677-687.

[7] Blajer, W., Dziewiecki, K., and Mazur, Z., 2007, "Multibody Modeling of Human Body for the Inverse Dynamics Analysis of Sagittal Plane Movements," Multibody System Dynamics, 18(2), pp. 217-232.

[8] Lu, L., 2007, "Inverse Modelling and Inverse Simulation for System Engineering and Control Applications," Ph.D. thesis, Ph. D. Thesis, Faculty of Engineering, University of Glasgow,

[9] Murray-Smith, D. J., 2011, "Feedback Methods for Inverse Simulation of Dynamic Models for Engineering Systems Applications," Mathematical and Computer Modelling of Dynamical Systems, 17(5), pp. 515-541.

[10] Blajer W., G. J., Krawczyk M.,, 2001, "Prediction of the Dynamic Characteristics and Control of Aircraft in Prescribed Trajectory Flight," Journal of theoretical and applied mechanics, 39(1), pp. 79-103.

[11] Celi, R., 2000, "Optimization-Based Inverse Simulation of a Helicopter Slalom Maneuver," Journal of Guidance, Control, and Dynamics, 23(2), pp. 289-297.

[12] Öström, J., 2007, "Enhanced Inverse Flight Simulation for a Fatigue Life Management System," eds., Hilton Head, SC, 1, pp. 60-68.

[13] Doyle, S. A., and Thomson, D. G., 2000, "Modification of a Helicopter Inverse Simulation to Include an Enhanced Rotor Model," Journal of Aircraft, 37(3), pp. 536-538.

[14] De Divitiis, N., 1999, "Inverse Simulation of Aeroassisted Orbit Plane Change of a Spacecraft," Journal of Spacecraft and Rockets, 36(6), pp. 882-889.
[15] Gu, X., Renaud, J. E., Batill, S. M., Brach, R. M., and Budhiraja, A. S., 2000, "Worst Case Propagated Uncertainty of Multidisciplinary Systems in Robust Design Optimization," Structural and Multidisciplinary Optimization, 20(3), pp. 190-213.
[16] Chen, W., Jin, R., and Sudjianto, A., 2005, "Analytical Variance-Based Global Sensitivity Analysis in Simulation-Based Design under Uncertainty," Journal of Mechanical Design, Transactions of the ASME, 127(5), pp. 875-886.
[17] Oberkampf, W. L., Deland, S. M., Rutherford, B. M., Diegert, K. V., and Alvin, K. F., 2002, "Error and Uncertainty in Modeling and Simulation," Reliability Engineering and System Safety, 75(3), pp. 333-357.
[18] Zhang, X. Y., Jin, X. L., Qi, W. G., and Guo, Y. Z., 2008, "Vehicle Crash Accident Reconstruction Based on the Analysis 3d Deformation of the Auto-Body," Advances in Engineering Software, 39(6), pp. 459-465.
[19] Xianghai, C., Xianlong, J., Xiaoyun, Z., and Xinyi, H., 2011, "The Application for Skull Injury in Vehicle-Pedestrian Accident," International Journal of Crashworthiness, 16(1), pp. 11-24.
[20] Lei, G., Xian-Long, J., Xiao-Yun, Z., Jie, S., Yi-Jiu, C., and Jian-Guo, C., 2008, "Study of Injuries Combining Computer Simulation in Motorcycle-Car Collision Accidents," Forensic Science International, 177(2-3), pp. 90-96.
[21] Kokkolaras, M., Mourelatos, Z. P., and Papalambros, P. Y., 2006, "Design Optimization of Hierarchically Decomposed Multilevel Systems under Uncertainty," Journal of Mechanical Design, Transactions of the ASME, 128(2), pp. 503-508.
[22] Zou, T., Cai, M., Du, R., and Liu, J., "Analyzing the Uncertainty of Simulation Results in Accident Reconstruction with Response Surface Methodology," Forensic Science International, pp.
[23] Wach, W., and Unarski, J., 2007, "Uncertainty of Calculation Results in Vehicle Collision Analysis," Forensic Science International, 167(2-3), pp. 181-188.
[24] Du, X., 2012, "A Reliability Approach to Inverse Simulation under Uncertainty," The ASME 2012 International Design Engineering Technical Conferences (IDETC) and Computers and Information in Engineering Conference (CIE), ASME, Chicago.

[25] Chen, W., Baghdasaryan, L., Buranathiti, T., and Cao, J., 2004, "Model Validation Via Uncertainty Propagation and Data Transformations," AIAA Journal, 42(7), pp. 1406-1415.
[26] Liu, Y., Chen, W., Arendt, P., and Huang, H. Z., 2011, "Toward a Better Understanding of Model Validation Metrics," Journal of Mechanical Design, Transactions of the ASME, 133(7), pp.
[27] Youn, B. D., Jung, B. C., Xi, Z., Kim, S. B., and Lee, W. R., 2011, "A Hierarchical Framework for Statistical Model Calibration in Engineering Product Development," Computer Methods in Applied Mechanics and Engineering, 200(13-16), pp. 1421-1431.
[28] Chen, W., Xiong, Y., Tsui, K. L., and Wang, S., 2008, "A Design-Driven Validation Approach Using Bayesian Prediction Models," Journal of Mechanical Design, Transactions of the ASME, 130(2), pp.
[29] Chen, W., Yin, X., Lee, S., and Liu, W. K., 2010, "A Multiscale Design Methodology for Hierarchical Systems with Random Field Uncertainty," Journal of Mechanical Design, Transactions of the ASME, 132(4), pp. 0410061-04100611.
[30] Drignei, D., Mourelatos, Z., Kokkolaras, M., Li, J., and Koscik, G., 2011, "A Variable-Size Local Domain Approach to Computer Model Validation in Design Optimization," SAE International Journal of Materials and Manufacturing, 4(1), pp. 421-429.
[31] Ferson, S., and Oberkampf, W. L., 2009, "Validation of Imprecise Probability Models," International Journal of Reliability and Safety, 3(1-3), pp. 3-22.
[32] Ferson, S., Oberkampf, W. L., and Ginzburg, L., 2008, "Model Validation and Predictive Capability for the Thermal Challenge Problem," Computer Methods in Applied Mechanics and Engineering, 197(29-32), pp. 2408-2430.
[33] Xiong, Y., Chen, W., and Tsui, K. L., 2008, "A New Variable-Fidelity Optimization Framework Based on Model Fusion and Objective-Oriented Sequential Sampling," Journal of Mechanical Design, Transactions of the ASME, 130(11), pp. 1114011-1114019.
[34] Xi, Z., Youn, B. D., and Hu, C., 2010, "Random Field Characterization Considering Statistical Dependence for Probability Analysis and Design," Journal of Mechanical Design, Transactions of the ASME, 132(10), pp.
[35] Goda, K., 2010, "Statistical Modeling of Joint Probability Distribution Using Copula: Application to Peak and Permanent Displacement Seismic Demands," Structural Safety, 32(2), pp. 112-123.

[36] Noh, Y., Choi, K. K., and Du, L., 2009, "Reliability-Based Design Optimization of Problems with Correlated Input Variables Using a Gaussian Copula," Structural and Multidisciplinary Optimization, 38(1), pp. 1-16.

[37] Choi, S. K., Grandhi, R. V., and Canfield, R. A., 2007, *Reliability-Based Structural Design*, Springer,

[38] Eldred, M. S., and Burkardt, J., 2009, "Comparison of Non-Intrusive Polynomial Chaos and Stochastic Collocation Methods for Uncertainty Quantification," eds., pp.

[39] Sudret, B., 2008, "Global Sensitivity Analysis Using Polynomial Chaos Expansions," Reliability Engineering and System Safety, 93(7), pp. 964-979.

[40] Chen, W., Tsui, K.-L., Allen, J. K., and Mistree, F., 1995, "Integration of the Response Surface Methodology with the Compromise Decision Support Problem in Developing a General Robust Design Procedure," eds., 82, pp. 485-492.

List of Table Captions

List of Figure Captions

Table 1 Output variables and distributions of random input variables

Variable	y_1	y_2	$x_{\mathrm{rand},\,1}$	$x_{\mathrm{rand},\,2}$
Distribution Type	Deterministic	Deterministic	Normal	Normal
Mean	1	5	1	1
Standard Deviation	0	0	0.5	0.5

Table 2. Parameters and variables of the traffic accident reconstruction problem

Variable	S_x (m)	S_y (m)	v (km/h)	d (m)	μ_k
Distribution Type	Deterministic	Deterministic	Deterministic	Normal	Normal
Mean	9.59	17.02	[40, 100]	0.4	0.7
Standard Deviation	0	0	0	0.2	0.1

Table 3. Samples and simulation results

	d (m)	v （km/h）	μ_k	(s_x, s_y) (m)
1	0.3900	100.000	0.6569	（43.80, 7.68）
2	0.2651	98.000	0.7431	（27.96, 10.96）
3	0.5049	96.000	0.5779	（37.46, 15.31）
4	0.1599	94.000	0.6860	（21.85, 11.32）
5	0.4637	92.000	0.7765	（15.56, 12.46）
6	0.3363	90.000	0.6235	（25.39, 9.13）
7	0.6601	88.000	0.7140	（15.50, 19.47）
8	0.1132	86.000	0.8221	（19.91, 10.99）
9	0.4315	84.000	0.5214	（33.42, 16.29）
10	0.3022	82.000	0.6669	（23.29, 11.54）
11	0.5274	80.000	0.7535	（13.03, 12.99）
12	0.2226	78.000	0.5956	（17.51, 10.95）
13	0.4878	76.000	0.6954	（21.63, 14.68）
14	0.4185	74.000	0.7986	（13.65, 12.94）
15	0.7168	72.000	0.6354	（5.75, 15.96）
16	0.0275	70.000	0.7234	（16.17, 11.17）
17	0.4257	68.000	0.8446	（7.90, 14.63）
18	0.2842	66.000	0.5554	（11.00, 9.97）
19	0.5553	64.000	0.6766	（10.92, 11.90）
20	0.1980	62.000	0.7646	（8.05, 11.55）
21	0.4905	60.000	0.6104	（7.74, 11.55）
22	0.4026	58.000	0.7046	（9.24, 11.89）
23	0.6636	56.000	0.8044	（-3.18, 14.59）
24	0.1364	54.000	0.6465	（3.22, 11.46）
25	0.4874	52.000	0.7331	（1.25, 12.68）
26	0.3195	50.000	0.8786	（0.45, 11.67）
27	0.6020	48.000	0.4754	（-1.81, 15.07）
28	0.2847	46.000	0.6603	（2.24, 10.49）
29	0.5158	44.000	0.7465	（0.10, 11.34）
30	0.3843	42.000	0.5842	（2.94, 9.96）

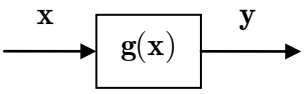

Figure 1. A simulation model

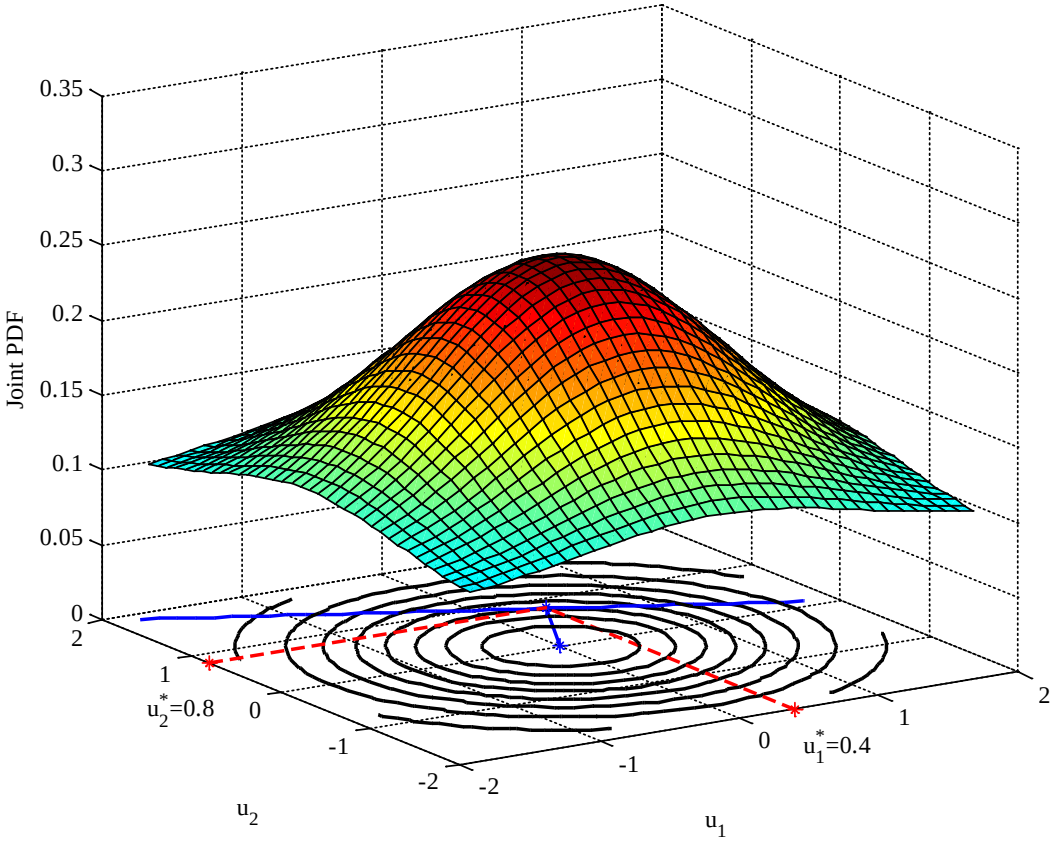

Figure 2. Joint PDF of u_1 and u_2

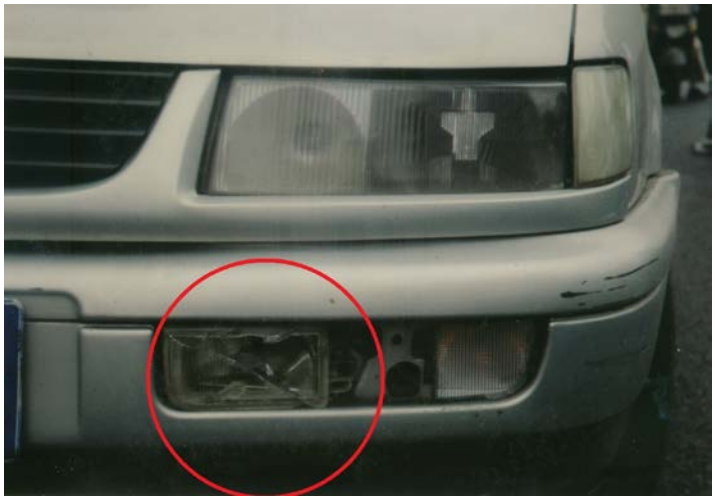

Figure 3. Bumper damage

Figure 4. Windscreen damage

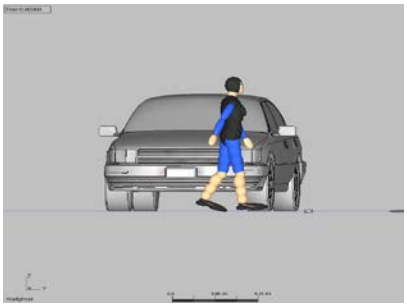

(a) Front view

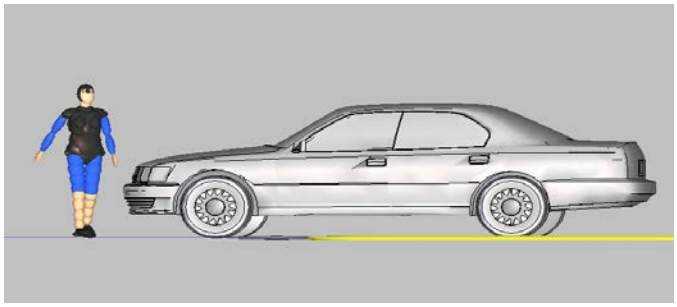

(b) Side view

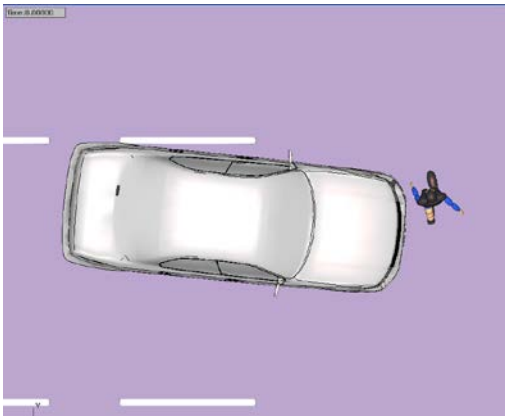

(c) Top view

Figure 5. 3D simulation of the accident

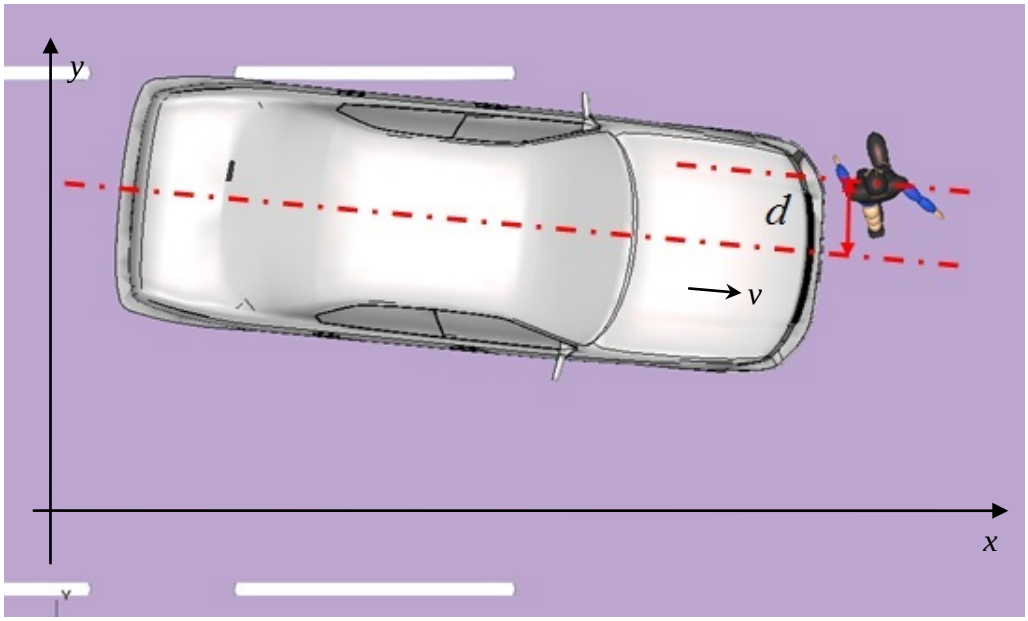

Figure 6. Simulation parameters

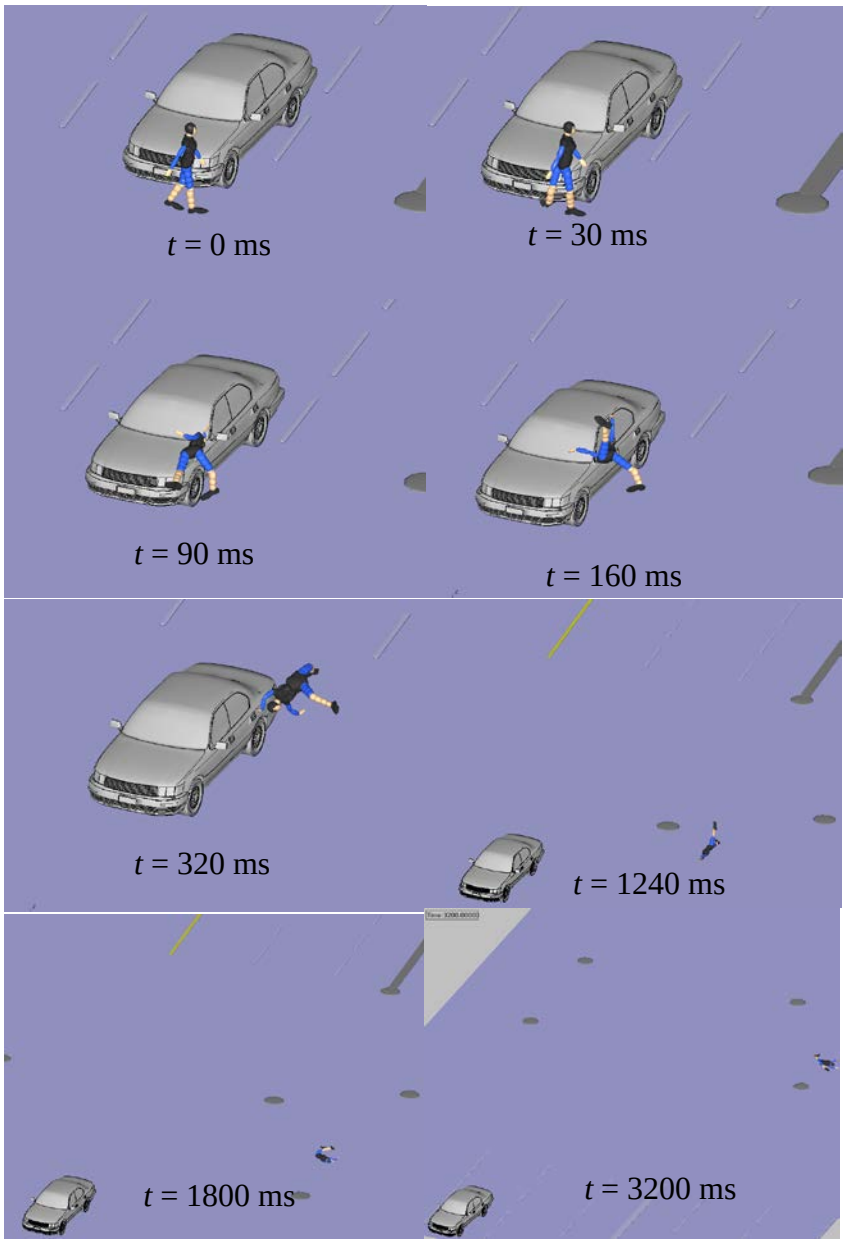

Figure 7. Vehicle accident simulation

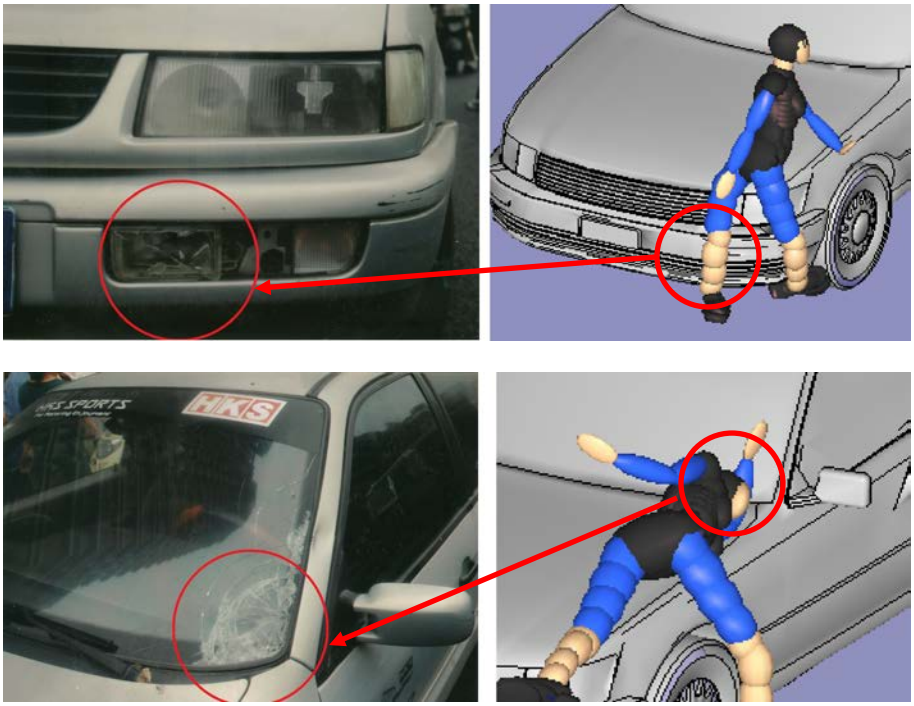

Figure 8. Pedestrian's injury and deformation of vehicle body

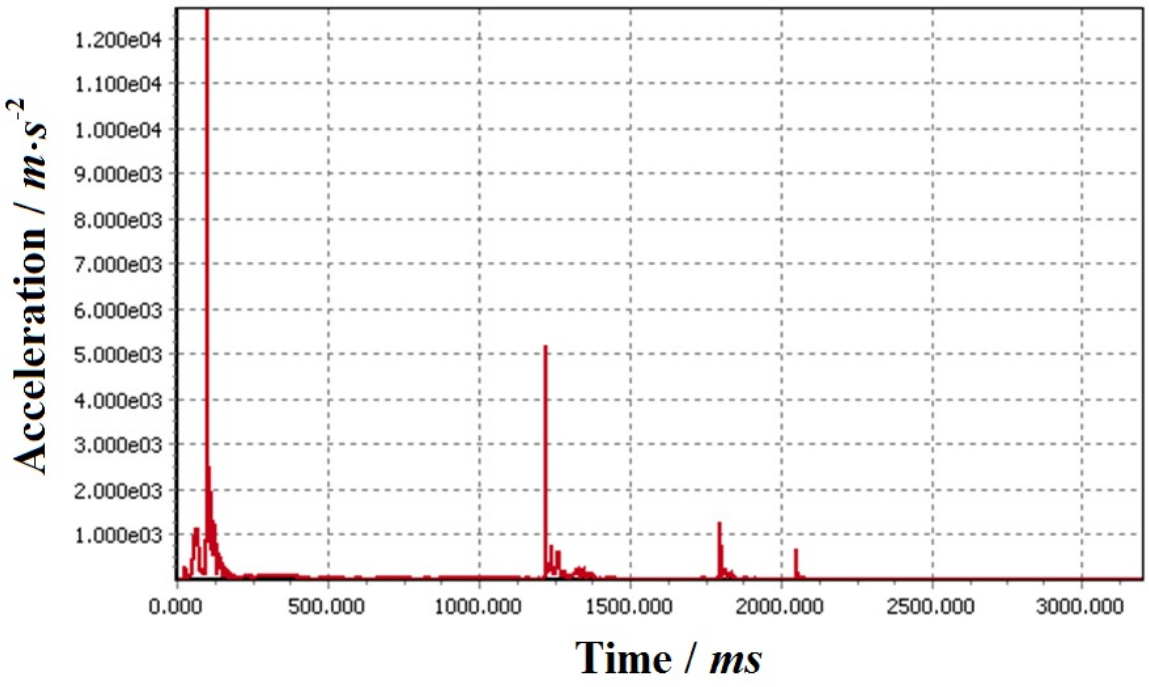

Figure 9. Acceleration of the pedestrian's head

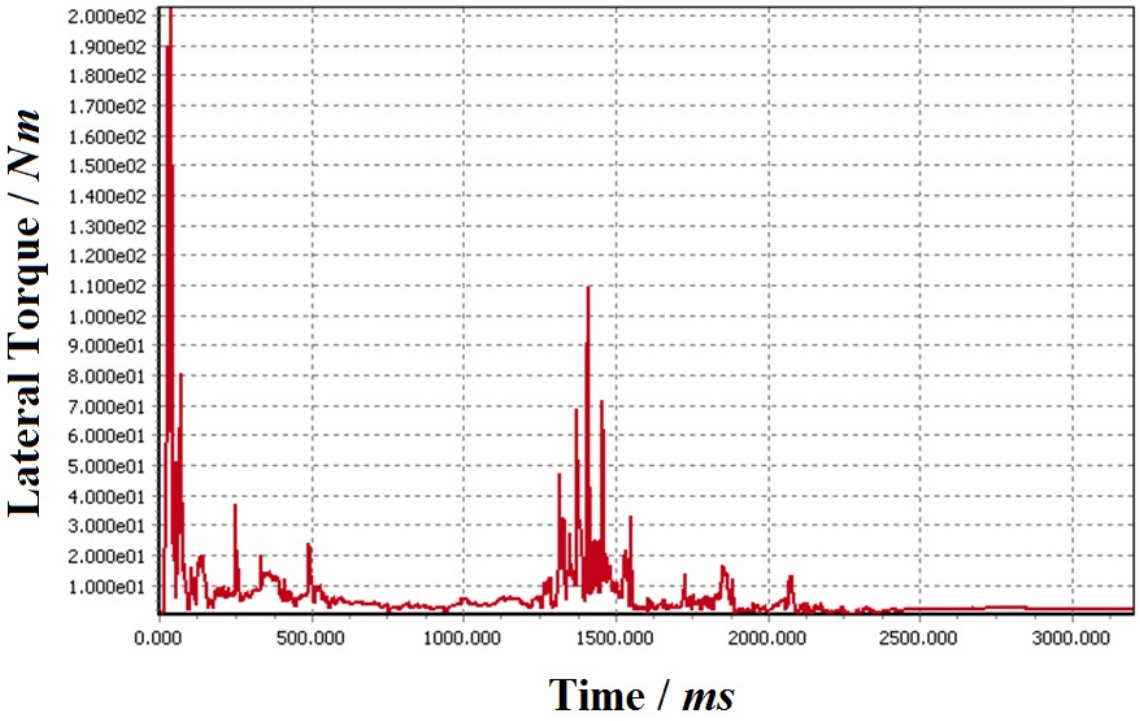

Figure 10. Lateral Torque of the pedestrian's lower limbs